

Mtg16/Eto2 Contributes to Murine T-Cell Development^{∇†}

Aubrey Hunt,¹ Melissa Fischer,¹ Michael E. Engel,^{2,3,4,5} and Scott W. Hiebert^{1,5*}

Department of Biochemistry,¹ Department of Pediatrics,² and Department of Cancer Biology,³ Vanderbilt University School of Medicine, Nashville, Tennessee, and Monroe Carell Jr. Children's Hospital⁴ and Vanderbilt-Ingram Cancer Center,⁵ Vanderbilt University Medical Center, Nashville, Tennessee

Received 21 December 2010/Returned for modification 7 February 2011/Accepted 22 April 2011

Mtg16/Eto2 is a transcriptional corepressor that is disrupted by t(16;21) in acute myeloid leukemia. Using mice lacking *Mtg16*, we found that *Mtg16* is a critical regulator of T-cell development. Deletion of *Mtg16* led to reduced thymocyte development *in vivo*, and after competitive bone marrow transplantation, there was a nearly complete failure of *Mtg16*^{-/-} cells to contribute to thymocyte development. This defect was recapitulated *in vitro* as *Mtg16*^{-/-} Lineage⁻/Sca1⁺/c-Kit⁺ (LSK) cells of the bone marrow or DN1 cells of the thymus failed to produce CD4⁺/CD8⁺ cells in response to a Notch signal. Complementation of these defects by reexpressing *Mtg16* showed that 3 highly conserved domains were somewhat dispensable for T-cell development but required the capacity of *Mtg16* to suppress E2A-dependent transcriptional activation and to bind to the Notch intracellular domain. Thus, *Mtg16* integrates the activities of signaling pathways and nuclear factors in the establishment of T-cell fate specification.

The progeny of hematopoietic stem cells receive external signals and integrates them into altered transcriptional programs that direct multipotent progenitor cells to become lineage committed and generate all the mature cell types found in the peripheral blood (29, 37). Development along these distinct lineages requires that the external cues be faithfully interpreted at the transcriptional level to activate and repress lineage-specific gene expression programs (27, 32). Transcriptional coactivators and corepressors are ideally situated to integrate the activities of multiple DNA binding transcription factors and signaling pathways to alter gene expression programs and regulate lineage allocation (8, 23).

Myeloid translocation gene (MTG) 16 (*MTG16*) is disrupted by the t(16;21) in acute myeloid leukemia (AML) (17). *MTG16* (gene name *CBFA2T3*; also known as *ETO2*) is a member of a family of transcriptional corepressors that also includes *MTGR1* and *MTG8* (also known as *ETO*), the latter of which is targeted by t(8;21) (15, 25, 33). These translocations fuse the DNA-binding domain of *RUNX1* to nearly all of either *MTG16* or *MTG8* to repress the transcription of *RUNX1*-regulated genes (15, 17, 18, 33). As expected for corepressors, *MTG16* binds to both DNA binding proteins and chromatin-modifying factors (1, 9, 14, 19, 34, 41). Four highly homologous domains within *MTGs* are evolutionarily conserved in the *Drosophila melanogaster* factor Nery and mediate some of these contacts.

The action of E proteins and Notch signaling are critical to T-cell development, and a potential role for *Mtg16* in lymphopoiesis was further suggested by the identification of an association between *MTGs* and these pathways (9, 14, 19, 38, 41,

48). Upon ligand binding, the Notch receptor is cleaved and the intracellular domain (ICD) of Notch moves to the nucleus and binds the transcription factor CBF1-Suppressor of Hairless-Lag1 (CSL) to activate transcription (26). *MTGs* appear to act as corepressors for CSL, and independent of CSL, *Mtg16* also associates with the Notch ICD, suggesting that *Mtg16* mediates some aspects of Notch functions (14, 38).

Likewise, *Mtg16* associates with transcriptional activation domain 1 (AD1) in E proteins to impair E-protein-dependent transcription, and E2A instructs lymphoid development while inhibiting myelopoiesis (2, 3, 7, 35, 48). *E2A*-null mice have decreased numbers of thymocytes due to reduced lymphoid-primed multipotent progenitor (LMPP) and early thymocyte progenitor (ETP) production and impaired progression from the earliest CD4⁻ CD8⁻ CD44⁺ CD25⁻ double-negative 1 (DN1) thymocytes to the subsequent CD4⁻ CD8⁻ CD44⁺ CD25⁺ DN2 thymocytes (2, 4, 13, 24). Furthermore, *E2A*-null progenitor cells fail to produce T cells in *in vitro* cell fate specification assays initiated by Notch signaling (21, 39). Here, we show that inactivation of *Mtg16* impairs the development of T-cell lineage thymocytes, indicating that *Mtg16* has the capacity to interact with key factors that specify the T-cell lineage, potentially serving as a master regulator of this cell fate decision.

MATERIALS AND METHODS

Mice. Generation of *Mtg16*-null mice was previously described (10). For studies described here, *Mtg16*-null mice were backcrossed into the C57BL/6 background for 10 generations.

Plasmids. The E-protein-deficient *Mtg16* point mutant plasmids were generated using a QuikChange II XL site-directed mutagenesis kit (Agilent Technologies). Primers were designed based upon the structure of the Eto-HEB interaction (35) to mimic the following mutations: F210A-F154A and R220A-R164A. The sequence for the F210A forward primer was 5'-CACTGAGGCCGTTTGT TATCCTGCTCTGAAGGCTAATCTT-3', and that for the F210A reverse primer was 5'-AAGATTAGCCTTCAGAGCAGGATAACAACGGCCTC AGTG-3'. The sequence for the R220A forward primer was 5'-CTTCCACTG CTGCAGGCTGAGCTCTGCACTG-3', and that for the R220A reverse primer was 5'-CAGTGCAGGAGCTCAGCCTGCAGCAGTGGAAAG-3'. Murine stem cell virus (MSCV)-*Id1* and MSCV-*Id2* were generous gifts of Jonathan

* Corresponding author. Mailing address: Department of Biochemistry, 512 Preston Research Building, Vanderbilt University School of Medicine, 2220 Pierce Ave., Nashville, TN 37232. Phone: (615) 936-3582. Fax: (615) 936-1790. E-mail: scott.hiebert@vanderbilt.edu.

† Supplemental material for this article may be found at <http://mc.manuscriptcentral.com/mcb>.

∇ Published ahead of print on 2 May 2011.

Keller. Fragments of Mtg16 deleted from the 5' or 3' ends were generated by PCR amplification and assembled in appropriate combinations to create Δ NHR1, Δ NHR2, Δ NHR3, Δ NHR4, Δ PST2, and Δ NHR1-PST2 interstitial deletion mutants. Fragments were subcloned into EcoRI/XhoI-restricted MSCV or pCMV5 for use in terminal experiments. The primer sequences and amplicon combinations used to create these Mtg16 interstitial deletion mutants are available upon request. The regions deleted in each mutant were as follows: Δ NICD deleted amino acids 1 to 85, Δ NHR1 deleted amino acids 145 to 242, Δ NHR2 deleted amino acids 365 to 402, Δ NHR3 deleted amino acids 460 to 510, Δ NHR4 deleted amino acids 532 to 567, Δ PST2 deleted amino acids 242 to 364, and Δ NHR1-PST2 deleted amino acids 145 to 364.

Cell culture and expression analysis. Bosc23, Cos7, and 293T cells were cultured in Dulbecco's modified Eagle Medium (DMEM) supplemented with 10% fetal bovine serum (FBS), 50 U/ml penicillin, 50 μ g/ml streptomycin, and 2 mM L-glutamine. OP9-DL1 stromal cells were cultured in α -MEM (Gibco) supplemented with 20% heat-inactivated FBS, 50 U/ml penicillin, and 50 μ g/ml streptomycin. Expression from MSCV-IRES-GFP plasmids was confirmed after transfection of 3 μ g of plasmid into Bosc23 virus-producing cells with PolyFect (Qiagen). At 48 h posttransfection, cells were harvested into radioimmunoprecipitation assay (RIPA) buffer containing protease inhibitors, diluted 1:2 in Laemmli's sample buffer (Bio-Rad), sonicated, and subjected to 10% sodium dodecyl sulfate-polyacrylamide gel electrophoresis. Immunoblot analyses were performed using anti-Myc 9E10 antibody, with glyceraldehyde-3-phosphate dehydrogenase (GAPDH) expression (AbCam) as a loading control. Expressed proteins were visualized using fluorophore-conjugated secondary antibodies and the Odyssey system (LiCor).

Flow cytometry and cell sorting. Single-cell suspensions were formed after the tibia and/or femur was flushed with phosphate-buffered saline (PBS) to collect bone marrow cells or after the spleen or thymus was minced into fragments and passed through a 70- μ m filter. Antibody staining for flow cytometry was carried out on 1×10^6 cells in single wells of a round-bottom 96-well plate. For lineage labeling, cells were stained with biotinylated antibodies directed toward lineage-specific cell surface markers (CD3, B220, Gr1, Mac1, and Ter119; eBioscience), followed by fluorochrome-conjugated streptavidin. For all other flow cytometry experiments, cells were labeled with the appropriate combination of fluorochrome-conjugated anti-c-Kit, anti-Sca-1, anti-Flt3, anti-CD44, anti-CD25, anti-CD4, anti-CD8, anti-Gr1, anti-Mac1, anti-B220, anti-CD45.2, and anti- $\gamma\delta$ T-cell receptors (eBioscience). Analysis was performed with a 3-laser BD LSR II using FACSDiva software. For rare populations of cells, bone marrow samples were first lineage depleted using a lineage depletion kit and magnetic cell sorting (Miltenyi Biotec). For rare populations of thymic progenitor cells, total cell suspensions were first lineage depleted using the eBioscience lineage panel plus anti-CD4-biotin and anti-CD8-biotin and magnetic cell sorting (Miltenyi Biotec). Sorting of hematopoietic cell populations was performed on a BD FACSAria.

Competitive bone marrow transplants. For competitive reconstitution assays, a single-cell suspension of bone marrow cells was obtained from the tibia and femur, and the red blood cells were lysed with erythrocyte lysis buffer (buffer EL; Qiagen). Bone marrow cells were injected via the tail vein into lethally irradiated (900 rads) recipient C57BL/6 CD45.1 congenic mice. The Mtg16^{+/+} or Mtg16-null donor cells were mixed with C57BL/6 CD45.1 bone marrow cells (9:1). The reconstitution potential of the donor (CD45.2) cells was monitored by flow cytometry of the peripheral blood and/or the bone marrow, thymus, and spleen.

Gene expression analysis. The expression of individual genes was measured using reverse transcriptase (RT) PCR, with total RNA isolated using a 5 Prime PerfectPure RNA extraction kit. The RT step was carried out using 100 to 200 ng total RNA per 20 μ l of iScript (Bio-Rad) cDNA synthesis reaction mixture; one-fourth of the reaction mixture was used for PCR using iQ Sybr green SuperMix (Bio-Rad), with GAPDH as an internal control. PCRs were performed in duplicate. The primer sequences were as follows: mMtg8F, 5'-ATTTACGC CAACGACATTAACGA-3'; mMtg8R, 5'-CTGAGTTGCTAGCACCACA-3'; mMtgr1F, 5'-ACCTGGCCAGCATGAGC-3'; mMtgr1R, 5'-AATGTCTT CTAGTGTATAGTGC-3'; mMtg16F, 5'-CCACGGCTGCTTAAAGTGGT-3'; mMtg16R, 5'-GTCATTGCCAAATTGCTGTAGG-3' GAPDH, 5'-GCCTTC CGTGTTCCTACCC-3'; and GAPDHR, 5'-TGCCTGCTTACCACCTTC-3'.

In vitro differentiation assays. The indicated sorted populations of cells were plated on irradiated, confluent OP9-DL1 stromal cells in α -MEM (Gibco) supplemented with 20% FBS, 50 U/ml penicillin, 50 μ g/ml streptomycin, 5 ng/ml interleukin-7 (IL-7; Peprotech), and 5 ng/ml Flt3 ligand (Peprotech). The hematopoietic cells were collected and passaged every 4 to 7 days onto a fresh stromal layer. T-cell differentiation was assessed every 7 days for 4 weeks by flow cytometry.

Cell cycle analysis. Cell cycle analysis of hematopoietic cells cocultured with OP9-DL1 cells was performed using propidium iodide staining of genomic DNA.

Collected cells were fixed in 70% ethanol (EtOH) overnight and treated with 0.1% Triton X-100, 20 μ g/ml propidium iodide (Sigma), and 0.1 mg/ml RNase A (USB) in phosphate-buffered saline (PBS) prior to fluorescence-activated cell sorter (FACS) analysis.

Annexin V staining. Annexin V analysis of hematopoietic cells cocultured with OP9-DL1 stromal cells was performed using annexin V-fluorescein isothiocyanate (annexin V-FITC) apoptosis detection kit I (BD Pharmingen) per the manufacturer's instructions. Briefly, cells were collected from day 7 cultures, washed in PBS, and counted. Cells were resuspended in annexin V binding buffer, labeled with annexin V-FITC, and then analyzed by flow cytometry.

Retroviral expression. MSCV-myc-Eto2-GFP and variants, MSCV-Id1-GFP, and MSCV-Id2-GFP were transfected into Bosc23 virus-producing cells. The viral supernatant was collected at 48 h posttransfection and filtered through a 45- μ m syringe filter (Nalgene). Sorted Lineage⁻/Sca1⁺/c-Kit⁺ (LSK) cells were centrifuged at 1,500 rpm for 1 h at room temperature with the viral supernatant prior to coculture with OP9-DL1 stromal cells. Infection was monitored using flow cytometry to detect green fluorescent protein (GFP) expression.

Transcription assays. Luciferase reporter assays were performed with 293T cells transfected with the indicated plasmids. Luciferase values were assessed from an E-box reporter plasmid, a generous gift of Robert Roeder. At 48 h posttransfection, cells were lysed with passive lysis buffer from the Promega Dual-Luciferase reporter assay system, and luciferase activity was measured on a BD Pharmingen Monolight 3010 luminometer. All experiments were performed in triplicate, and values were normalized to that of a *Renilla* luciferase internal control.

Coimmunoprecipitation assays. Cos7 cells were transfected with the indicated combinations of plasmids, and 40 h later, the cells were harvested into HERR buffer (100 mM KCl, 0.02 M HEPES, pH 7.9, 0.002 M EDTA, 0.1% NP-40, 10% glycerol) supplemented with a protease inhibitor cocktail (Roche). For Mtg16-E47 interactions, 600 mM KCl HERR was used. For Mtg16-Notch ICD interactions, 100 mM KCl HERR was used. Lysates were sonicated and cleared by centrifugation. Immunoprecipitation of lysates was performed using anti-c-Myc 9E10 antibody for Mtg16-E47 interactions and the Flag M2 antibody (Sigma) for Mtg16-NICD interactions. Immune complexes were collected using protein G-Sepharose 4B (Sigma). Coprecipitating proteins were identified by immunoblot analysis of immune complexes using anti-c-Myc 9E10, anti-Flag M2, and anti-E47 sc-763 antibodies (Santa Cruz).

RESULTS

Mtg16 is required for thymopoiesis after bone marrow transplantation. *Mtg16*-null mice are able to produce all of the hematopoietic lineages, though myeloid development is enhanced with increased numbers of Gr1⁺/Mac1⁺ myeloid cells in the spleen and bone marrow (see Fig. S1 in the supplemental material). However, there was a 2-fold decrease in total thymocyte number that was visible upon gross dissection (see Fig. S2A in the supplemental material), which caused us to examine T-cell development in more detail. Using flow cytometry, all populations were decreased in absolute number in the absence of *Mtg16* (see Fig. S2B in the supplemental material), with a small relative decrease in CD4⁺ CD8⁺ cells and a slight relative increase in CD4⁻ CD8⁻ cells and both CD4⁺ and CD8⁺ mature thymocytes as a percentage of total thymocytes. When the earliest thymocytes of the CD4⁻ CD8⁻ DN population were further subdivided using CD44 and CD25, there was a substantial decrease in both CD25⁻ CD44⁺ DN1 cells and CD25⁺ CD44⁺ DN2 cells in the absence of *Mtg16* (see Fig. S2C in the supplemental material). Consistent with the lower level of thymocytes, there were somewhat fewer $\gamma\delta$ T cells (by absolute number) (data not shown).

Our interest in the role of Mtg16 in T-cell development was heightened when we noted that after competitive bone marrow transplantation using 90% *Mtg16*^{-/-} CD45.2⁺ bone marrow cells and 10% control CD45.1-expressing cells, there was a dramatic loss of T-cell production from the null bone marrow

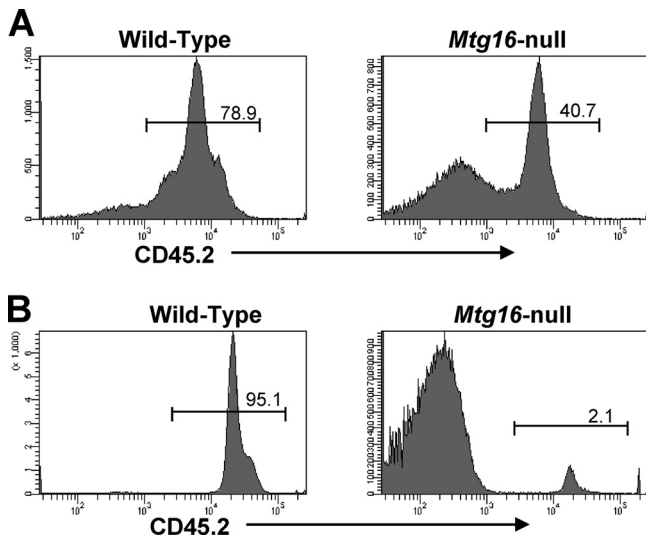


FIG. 1. *Mtg16* is required for thymopoiesis after bone marrow transplantation. *Mtg16*^{-/-} cells fail to repopulate the thymus in competitive transplant. Shown are representative CD45.2 FACS plots 6 weeks after bone marrow transplantation using 10% wild-type CD45.1 cells and 90% control or *Mtg16*^{-/-} CD45.2 cells. Representative FACS plots of cells harvested from the bone marrow (A) and thymus (B) are shown. These data are from one of two experiments, with a total of 5 WT recipients and 9 *Mtg16*-null recipients.

(Fig. 1A). As measured by flow cytometry, control CD45.2⁺ bone marrow showed robust reconstitution, which was similar to the percentage of CD45.2⁺ wild-type (WT) marrow transplanted. In contrast, only 2 to 3% of the thymocytes were derived from the *Mtg16*^{-/-} bone marrow (Fig. 1B). Thus, when homeostasis was disrupted and the null cells were placed in a competitive environment, *Mtg16* was required for T-cell formation *in vivo*.

To better interpret the defects in *Mtg16*-null early T-cell lineage progenitor cells, we measured the expression levels of *Mtg16* and the other MTG family members, *Mtg8* and *Mtgr1*, by quantitative RT-PCR in wild-type mice across several hematopoietic populations. The highest levels of *Mtg16* expression were seen in early stem/progenitor cell populations (LSK cells), common myeloid progenitors (CMPs), and bone marrow B220⁺ cells (see Fig. S3A in the supplemental material), whereas *Mtgr1* was widely expressed and *Mtg8* was poorly expressed, with undetectable expression in some populations. In the thymus, *Mtg16* expression levels were generally lower, with the highest levels in CD4⁺ CD8⁺ cells and lower levels in early T-cell progenitor cells. These data suggested that the defect in T-cell development might lie in the earliest T-cell progenitor cells of the bone marrow. Flow cytometric analysis supported this hypothesis and indicated that the lymphoid-primed multipotent progenitor cells (LMPP) of the bone marrow and the CD4⁻/CD8⁻/CD25⁻/c-Kit⁺ early thymocyte progenitor (ETP) cells that seed the thymus were reduced in the absence of *Mtg16* (Fig. 2A and B). The 2-fold reduction observed in progenitors was consistent with the 2-fold reduction observed in total thymocyte number (see Fig. S2A in the supplemental material).

Mtg16 is required for T-cell commitment *in vitro*. To directly assess the T-cell potential of *Mtg16*-null bone marrow progen-

itor cells and early thymocytes, we cultured wild-type and *Mtg16*-null bone marrow stem cells and thymus double-negative cells in the presence of Flt3 ligand and IL-7 on OP9 stromal cells expressing the Delta-like 1 Notch ligand, which triggers T-cell development (39). We isolated LSK cells as well as CD44⁺ CD25⁻ DN1 cells and CD44⁺ CD25⁺ DN2 cells from the thymus and assessed their abilities to develop into CD4⁺ CD8⁺ T cells using flow cytometry (39). Between days 21 and 28, wild-type LSK and DN1 cells produced CD4⁺ CD8⁺ T cells. As DN2 cells have already begun the process of committing to the T-cell lineage, CD4⁺ CD8⁺ T cells developed between days 7 and 14 (Fig. 3A). In contrast, *Mtg16*-null LSK and DN1 cells failed to develop into CD4⁺ CD8⁺ T cells (Fig. 3A). However, *Mtg16*-null DN2 cells developed into CD4⁺ CD8⁺ T cells within 7 to 14 days of culture on OP9-DL1 stroma, albeit at a reduced rate (Fig. 3A, right panels). The reduced numbers of T cells could reflect reduced proliferative capacity, as the null cells failed to expand to the levels of wild-type DN2 cells (see Fig. S4 in the supplemental material). Together, these data indicate that *Mtg16* is required for efficient T-cell development *in vivo* and *in vitro* and that this defect precedes lineage commitment into DN2 T cells of the thymus (Fig. 3A).

Given that the *Mtg16*-null LSK cells failed to develop into T cells, we determined their lineage fate in this *in vitro* system. Seven days after the initiation of the cultures, there was an exaggerated production of Gr1⁺/Mac1⁺ myeloid cells in the absence of *Mtg16* (Fig. 3B). These data suggest that *Mtg16*-null stem cells are incapable of developing along T-cell lineages *in vitro* and prefer to develop along myeloid lineages, even under conditions favorable for lymphoid development.

***Ex vivo* complementation of the *Mtg16*^{-/-} defect in T-cell development.** To begin to define how *Mtg16* functions in regulating T-cell development, we sought to complement the *Mtg16*-deficient T cells by exogenous expression of *Mtg16*. Recombinant murine stem cell virus (MSCV) expressing *Mtg16* and *GFP* was used to infect FACS-purified LSK cells, followed by culture with OP9-DL1 cells. Reexpression of *Mtg16* yielded T-cell differentiation typically producing from 7 to 30% CD4⁺ CD8⁺ cells in numerous biological replicates compared to the *Mtg16*-null cells infected with control MSCV (Fig. 4A and B). Therefore, the failure to differentiate into T cells was dependent on *Mtg16* rather than an off-target effect of the deletion.

Next, we utilized a panel of deletion mutants that removed each of the Nrvy homology regions (NHRs) in *Mtg16*. Each of these domains is highly conserved between MTG family members and facilitates interaction with different proteins, thereby allowing the identification of the crucial interactions that contribute to *Mtg16* functions. *Mtg16*-null LSK cells were infected with MSCV-IRES-*GFP*, MSCV-*Mtg16*-IRES-*GFP*, or deletion mutants of the conserved domains, and the cells were cultured on OP9-DL1 stroma in the presence of IL-7 and Flt3 ligand (see Fig. S5 in the supplemental material for the levels of expression). The *Mtg16* deletion mutant lacking NHR1 failed to complement the null phenotypes, whereas deletion of NHR2, NHR3, and NHR4 allowed reconstitution of T-cell development (Fig. 4B) but with somewhat lower efficiencies. Like Δ NHR1, deletion of a domain just upstream of NHR1, which mediates association with the Notch intracellular domain, Δ NICD, also failed to restore T-cell development. These

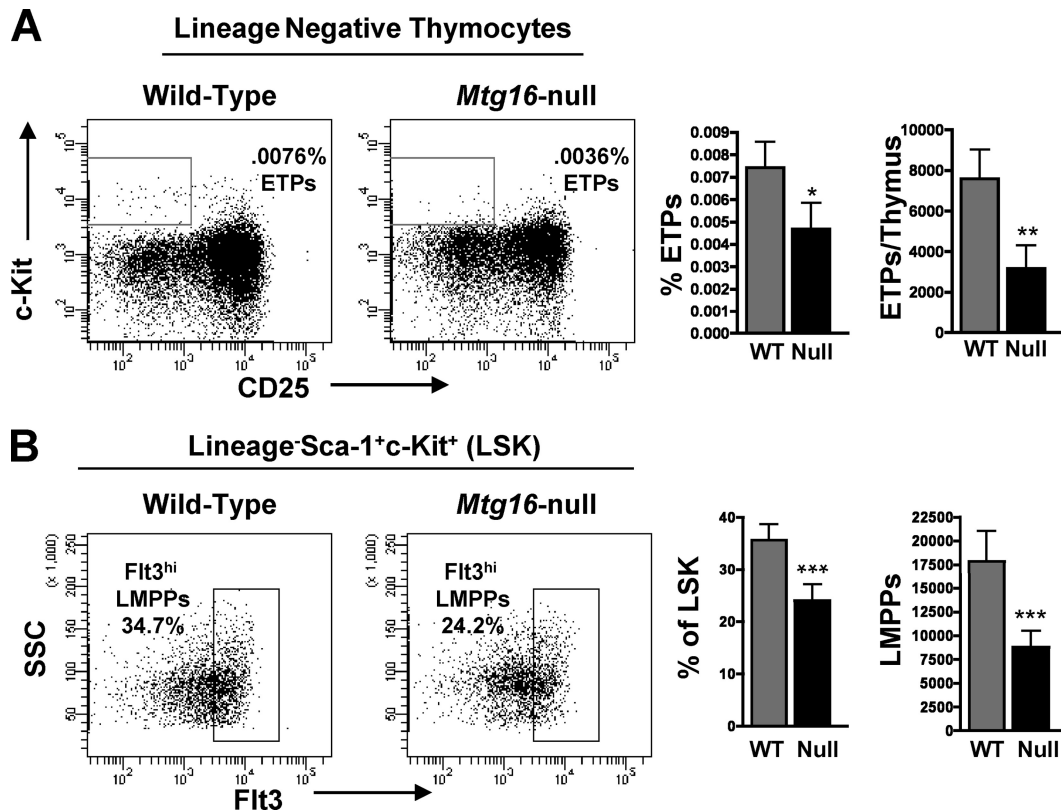


FIG. 2. Loss of *Mtg16* leads to decreased early thymocyte progenitor cells in the thymus and lymphoid-primed progenitor cells in the bone marrow. (A) Decreased presence of Lin⁻ CD25⁻ c-Kit⁺ ETPs in the *Mtg16*-null thymus shown both as percentages of total thymocytes and as absolute numbers per thymus \pm standard deviations (SD). Representative FACS plots are shown from one of three independent experiments with 4 mice of each genotype, with a total of 12 mice. An unpaired, two-tailed *t* test yielded *P* values of <0.05 (*) and <0.01 (**). (B) Decreased Lin⁻ Sca-1⁺ c-Kit⁺ Flt3^{hi} LMPs in *Mtg16*^{-/-} bone marrow shown both as percentages of LSKs and as absolute numbers per hind limb (both femur and tibia) \pm SD. Shown are data from a representative experiment with 5 mice of each genotype, with a total of 15 mice. An unpaired, two-tailed *t* test shows a *P* value of <0.001 (***)

results suggest that *Mtg16* must be able to associate with the NICD and specific transcription factors via NHR1 to fully regulate cell fate decisions.

E-protein regulation is necessary for the function of *Mtg16* in T-cell development. One of the interactions disrupted by the deletion of NHR1 is the interaction between this portion of *Mtg16* and activation domain 1 (AD1) of HEB (48). Given that the *Mtg16*-null phenotype is similar to that of *E2A*-deficient mice (2, 4, 13, 22), we mined gene expression data from *Mtg16*-null LSK cells (M. Fischer, I. Moreno-Miralles, A. Hunt, B. Chyla, and S. W. Hiebert, unpublished data) and found that *E2A* expression was slightly decreased, while the expression levels of *Id1* and *Id2*, negative regulators of E-protein DNA binding (6, 11, 44), were increased 4- to 8-fold. The expression of *Id1* in *in vitro* culture systems designed to permit B-cell development favored myeloid development over B-cell commitment (11). Because double short hairpin RNA (shRNA)-mediated knockdown of *Id1* and *Id2* was inefficient (data not shown), we asked whether the expression of *Id1* or *Id2* was sufficient to enhance myelopoiesis and block T-cell development in the OP9-DL1 system. MSCV-*Id1*-GFP- and MSCV-*Id2*-GFP-infected wild-type LSK cells were plated on OP9-DL1 stroma and FACS analyzed at day 7 to test for increased Gr1⁺/Mac1⁺ production, which was seen in the absence of

Mtg16. Both *Id1* and *Id2* overexpression led to increased myeloid production at day 7, suggesting that the increased expression of *Id1* and *Id2* in *Mtg16*-null LSK cells contributes to this phenotype (Fig. 5). Overexpression of *Id2* inhibited, but did not completely abolish, CD4⁺ CD8⁺ T-cell development in the OP9-DL1 assay (40). Similarly, we noted that *Id1*-expressing LSK cells also yielded some T-cell differentiation (Fig. 5B). Therefore, increases in *Id1* and *Id2* expression likely contribute to the enhanced myelopoiesis observed in the absence of *Mtg16* (Fig. 3B) but are unlikely to explain the block in T-cell differentiation.

The E proteins E2A and HEB are critical for T-cell development (2, 5). The structure of the NHR1 domain of MTG8 in association with the HEB AD1 domain identified residues that mediate this contact (35). While HEB binds to MTG8 through 2 sites, mutations within the NHR1 domain of MTG8 were sufficient to disrupt repression of E-protein-mediated transcriptional activation (20, 35). Therefore, to define the contributions of E-protein functions to the role of *Mtg16* in T-cell development, we engineered a point mutation in *Mtg16* that is homologous to changes that abrogated the binding of the MTG8 NHR1 domain to HEB AD1. The F210A *Mtg16* mutant mimics the F154A MTG8 mutant to eliminate E-protein AD1 binding, whereas a control R220A mutant mimics the

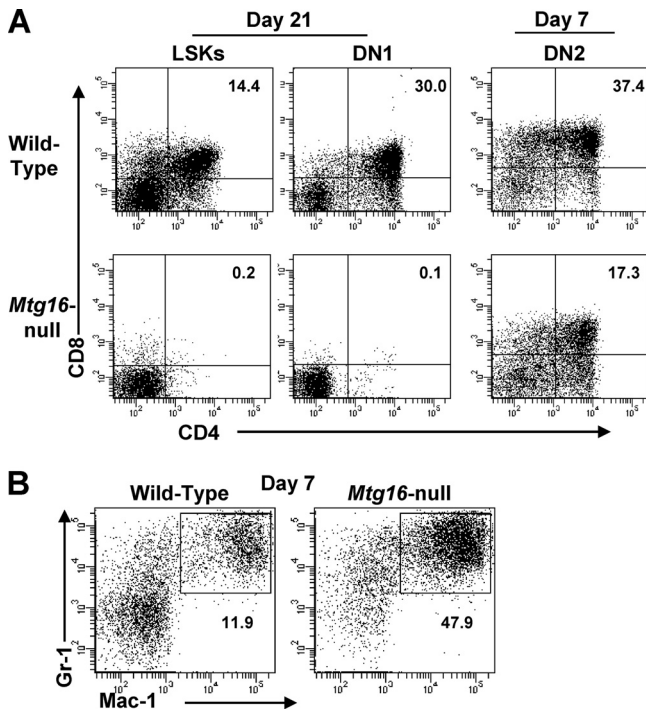


FIG. 3. *Mtg16*-null LSK and DN1 progenitor cells fail to develop into T cells *in vitro*. (A) FACS-sorted LSK, DN1, and DN2 populations were plated on OP9-DL1 cells, and CD4⁺ CD8⁺ T-cell development was assessed at day 21 for LSK and DN1 cells and day 7 for DN2 cells. Representative FACS plots are shown from one of at least two experiments. Shown are data from a representative experiment with 2 to 3 mice of each genotype, with a total of 5 (LSK), 7 (DN1), and 4 (DN2) mice. (B) *Mtg16*-null LSK cells display enhanced myelopoiesis. FACS plots for Gr1 and Mac1 7 days after culture of LSK cells with OP9-DL1 stromal cells are shown. Shown are data from a representative experiment from one of five independent experiments performed with 2 mice of each genotype, for a total of 10 mice.

R164A mutant that retained the ability to bind to HEB AD1 (35). The F210A and R220A mutants were reintroduced into *Mtg16*-null LSK cells using MSCV-IRES-GFP, and both *Mtg16* and the R220A mutant were capable of rescuing T-cell development (Fig. 6A). However, the F210A point mutant failed to rescue T-cell development (Fig. 6A). Therefore, appropriate regulation of E-protein activity is a necessary function of *Mtg16* in T-cell development.

Given that both deletion of the Notch ICD contact site and mutation of the E-protein binding motif impaired T-cell production, we probed the molecular contacts that these mutants retain. We confirmed that the point mutants in NHR1 did not disrupt E-protein binding and found that further deletion of a region between NHR1 and NHR2 (PST2 domain) was necessary to completely abrogate E-protein binding (see Fig. S6A and B in the supplemental material). The NHR1 domain of MTGs also contacts the nuclear receptor corepressor (NCoR) (45), but we found normal levels of repression by mutant GAL4-*Mtg16* fusion proteins using a Gal reporter assay (see Fig. S6D in the supplemental material). In addition, the F210A mutant retained the ability to bind to the Notch ICD (see Fig. S6C in the supplemental material), yet failed to properly respond to a Notch signal. Finally, we used a luciferase construct

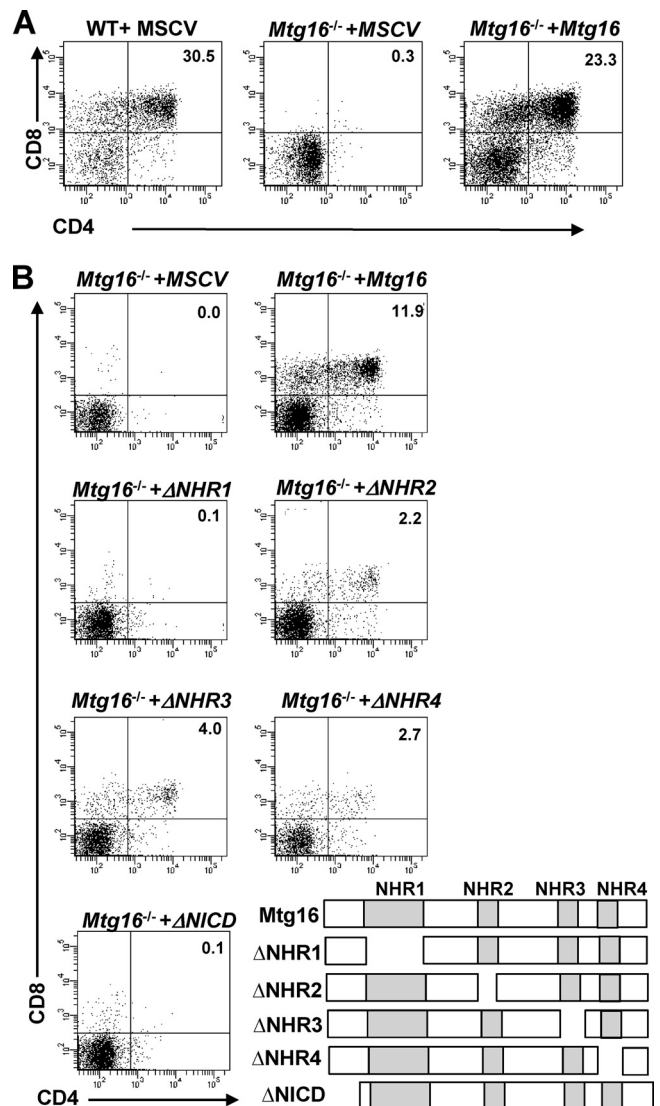


FIG. 4. Reconstitution of *Mtg16*^{-/-} LSK cells with *Mtg16* and *Mtg16* deletion mutants. (A) Representative FACS plots from day 21 cultures of LSK cells infected with MSCV or MSCV-*myc-Mtg16-GFP* cocultured with OP9-DL1 stroma to assess T-cell development using cell surface expression levels of both CD4 and CD8. GFP⁺ events are shown. Shown are data from a representative experiment from one of four independent experiments performed with 2 mice of each genotype, for a total of 8 mice. (B) Mutant analysis of *Mtg16* and contribution to T-cell development. Representative plots from day 21 cultures of LSK cells expressing MSCV or MSCV-*myc-Mtg16-GFP* on OP9-DL1 stroma assessing T-cell development by the cell surface expression levels of both CD4 and CD8. GFP⁺ events are shown. Shown are data from a representative experiment from one of two independent experiments performed with 2 control wild-type mice and 4 *Mtg16*^{-/-} mice pooled into two samples, for a total of 8 mice. A schematic diagram of the deletion mutants is shown in the lower right-hand portion. ΔNHR1, Δ145-242; ΔNHR2, Δ365-402; ΔNHR3, Δ460-510; ΔNHR4, Δ532-567; ΔNICD, Δ1-85.

carrying E-box binding sites in the promoter to show that *Mtg16* and *Mtg16*(R220A) suppressed E47-dependent transcriptional activation, while the F210A mutant was deficient in repression (Fig. 6B). Importantly, deletion of the N-terminal NICD binding region did not affect the ability of *Mtg16* to

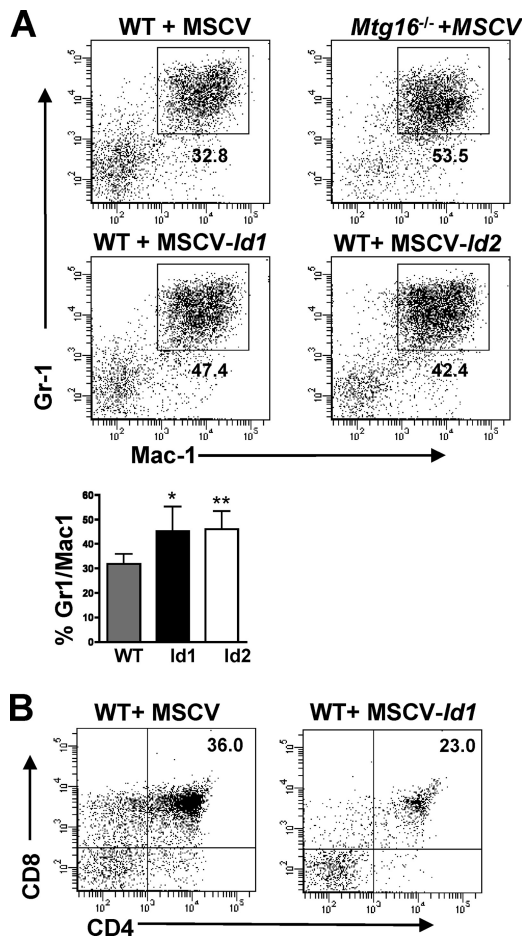


FIG. 5. Overexpression of *Id1* and *Id2* enhanced myeloipoiesis. (A) LSK cells infected with MSCV-*Id1*-GFP or MSCV-*Id2*-GFP phenocopy *Mtg16*^{-/-} LSK cells with increased production of Gr1⁺/Mac1⁺ cells. Representative FACS plots of GFP⁺ populations 7 days after coculture on OP9-DL1 stromal cells. Shown are GFP⁺ data from a representative experiment from one of two independent experiments performed with 2 to 3 mice of each genotype, for a total of 5 mice. The averages of the percentages of the cells that were Gr1⁺ Mac1⁺ that were obtained from two experiments are shown graphically in the panel below. An unpaired, two-tailed *t* test shows *P* values of <0.05 (*) and <0.01 (**). (B) WT LSK cells infected with MSCV-*Id1*-GFP retain the capacity to generate CD4⁺ CD8⁺ T cells after coculture on OP9-DL1 cells. Shown are GFP⁺ representative data from one of three experiments.

repress E47-mediated transcriptional activation (Fig. 6B), indicating that suppression of E-protein-dependent transcription was not sufficient to trigger T-cell development (Fig. 3) and that *Mtg16* must associate with the Notch ICD to restore function.

MTG family members function in transcriptional repression, and therefore, these results imply that E-protein-mediated repression contributes to T-cell development. By comparing gene expression profiles from *Mtg16*^{-/-} LSK cells (M. Fischer et al., unpublished) to those of genes that were repressed by overexpression of E47 (21, 42), we identified 19 genes that were repressed by E47 in hematopoietic progenitor cells but upregulated upon *Mtg16* inactivation in LSK cells (see Table S1 in the supplemental material). In addition, we compared

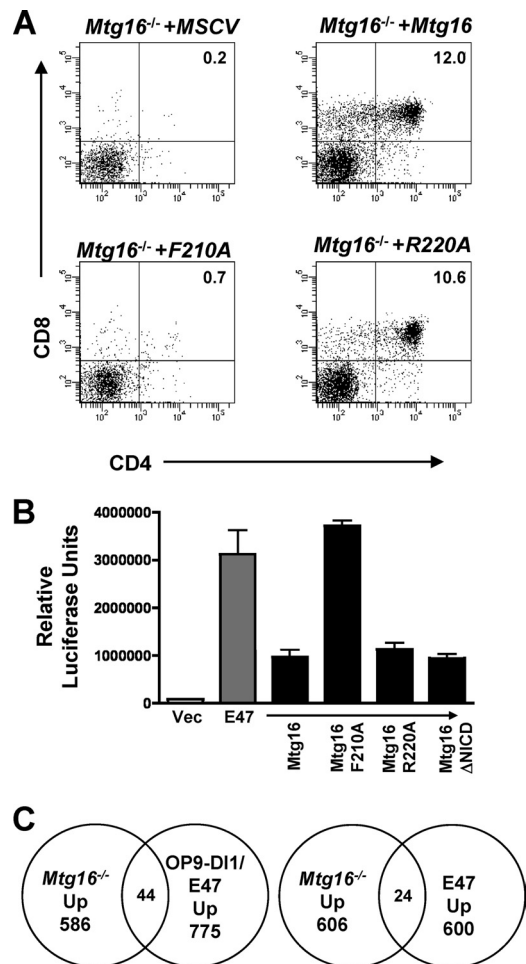


FIG. 6. Suppression of E-protein-mediated transcriptional activation is necessary for *Mtg16* to reconstitute T-cell development. (A) Retroviral introduction of wild-type MSCV-*myc*-*Mtg16*-GFP and the R220A mutant rescues CD4⁺ CD8⁺ T-cell development, but F210A does not. Representative day 21 FACS plots using anti-CD4 and anti-CD8 and with GFP⁺ cells shown. Shown are data from a representative experiment from one of three independent experiments performed with 2 mice of each genotype, for a total of 6 mice. (B) An F210A point mutant in *Mtg16* abrogates the ability of *Mtg16* to repress transcription from an E-box promoter activated by the expression of E47, while the NICD deletion mutant suppresses E-protein functions. The graph shows the average relative luciferase values ± SD from an E-box reporter plasmid cotransfected with a vector control or vector expressing E47 and the indicated *Mtg16* or *Mtg16* mutant thereof. The values were normalized to that of a *Renilla* luciferase plasmid to control for specificity and transfection efficiency. The experiment was performed twice in triplicate. (C) Venn diagrams are shown that display the intersection between genes upregulated in *Mtg16*^{-/-} LSK cells relative to wild-type controls and genes upregulated by activated Notch signaling in OP9-DL1 coculture and E47 expression (left panel) (21) or E2A-deficient thymic lymphoma cells that were complemented by reexpressing E47 (right panel) (42).

the changes in *Mtg16*^{-/-} gene expression profiles to those in genes regulated by overexpressed E47 in the context of Notch signaling from OP9-DL1 cells (see Table S2 in the supplemental material). A total of 44 genes that were upregulated by the loss of *Mtg16* were also coactivated by Notch signaling and E47 expression (Fig. 6C). Most importantly, key regulatory genes

were found within this group, including *Gata3*, *Id2*, *Socs3*, *Hes1*, and *Tle6*, which were also regulated by E47 in thymic lymphoma cells (42) (see Tables S3 and S4 in the supplemental material). Of note, the expression of *Mtg16*, but not *Mtg8* or *Mtgr1*, was activated by E47 (21), suggesting a possible regulatory loop between these proteins. Collectively, these data indicate that *Mtg16* plays a key role in integrating Notch signals and E-protein actions to suppress myelopoiesis and direct T-cell differentiation.

DISCUSSION

Our work indicates that *Mtg16* is required for lymphopoiesis after bone marrow transplantation and that it acts in the LSK and DN1 populations (Fig. 1 and 3). Surprisingly, 3 highly conserved domains, when deleted individually, were somewhat dispensable for *Mtg16* function in T-cell differentiation, even the oligomerization domain (Fig. 4, NHR2). In contrast, the Notch ICD interaction domain and the motif that is required for suppression of E-protein transactivation within NHR1 were required for *Mtg16* action (Fig. 4 and 6). Given the intersection between Notch signaling and E-protein function in T-cell differentiation, our data suggest that *Mtg16* is a key regulator of this process that contributes to maintaining the correct levels of several key genes that control lineage allocation and that are coordinately regulated by Notch signaling and E47 activation, including *Gata3*, *Id2*, and *Hes1* (see Tables S1 to S4 in the supplemental material).

Although the Notch ICD association motif was important for *Mtg16* function in T-cell development (Fig. 4), it is intriguing to note that *Mtg16*^{-/-} mice display many of the hallmarks of *E2A* deficiency. In addition to defects in T cells, mice lacking *E2A* contain reduced numbers of B cells, fewer long-term hematopoietic stem cells and multipotent progenitor cells, and fewer erythropoietic progenitor cells. In addition, stem cells lacking *E2A* showed a considerable defect in competitive repopulation assays (43, 47). Likewise, *Mtg16*^{-/-} mice show defective stress erythropoiesis with few erythropoietic progenitors, as measured by colony forming assays (10), and defects in stem cell competitiveness (M. Fischer et al., unpublished). Chromatin immunoprecipitation assays also suggest that the association between *Mtg16* and E proteins plays an important role in the action of these factors during hematopoiesis, as the most robust signal for *Mtg16* was found near E-protein binding sites (M. Fischer et al., unpublished).

While the NHR1 domain was essential, the NHR2 domain was not absolutely required for *Mtg16* function in the OP9-DL1 assay. NHR2 forms strong homo- and hetero-oligomers with MTG family members (25, 28, 30). In fact, other MTG family members were the major associating proteins when MTGs or RUNX1-MTG8 was purified (25, 48). Our analysis suggests that *Mtg16* monomers retain function, and the observation that Δ NHR1 and Δ NICD impaired *Mtg16* functions (Fig. 4) suggests that hetero-oligomers that might be formed with endogenous wild-type *Mtgr1* (the other MTG family member widely expressed in hematopoietic cells) (see Fig. S3 in the supplemental material) were unable to exert the same functions as *Mtg16* and thereby complement this defect. Similar to the NHR2 domain, the NHR3 and NHR4 domains were not absolutely required for *Mtg16* to rescue T-cell develop-

ment (Fig. 4). NHR4 mediates the weaker of the two contacts between *Mtg16* and NCoR/SMRT but is not required for association with NCoR or for transcriptional repression (1, 31), whereas the NHR3 domain contributes to binding the regulatory subunit of protein kinase A (PKA RII) (12, 16). Rather than contributing to the formation of acute leukemia, deletion of these domains has been associated with increasing the activity of the t(8;21) fusion protein (46), suggesting that these domains play a negative regulatory role.

Notch signaling is a key determinant in instructing T-cell development and, when coupled with IL-7, is sufficient to induce T-cell lineage development *in vitro* (36, 39). The Notch ICD binds to CSL and recruits Mastermind to activate transcription (26). The association of MTGs with CSL suggests that *Mtg16*, like *MTG8*, acts as a corepressor to suppress the expression of downstream target genes, such as *Hes1* (38). The discovery of an association between the Notch ICD and *Mtg16* furthered this model by suggesting a mechanism by which the Notch ICD impairs the association between *Mtg16* and CSL, perhaps allowing Mastermind to bind to CSL (14). The high levels of expression of the canonical Notch target genes *Hes1* and *Nrap* in *Mtg16*-null LSK cells (14) and the failure of the *Mtg16* mutant that lacks the Notch ICD binding motif to complement the null phenotype (Fig. 4), even though this mutant impaired E-protein-dependent transcriptional activation (Fig. 6B), are consistent with this interpretation. Importantly, our mutation data indicate that the loss of *Mtg16* perturbs the function of other necessary factors in T-cell development (e.g., E proteins) that allow the proper integration of Notch signals. Thus, *Mtg16* plays a critical role in integrating Notch signals and E-protein functions in T-cell development, perhaps in the earliest bone marrow progenitor cells.

ACKNOWLEDGMENTS

We thank the members of the Hiebert lab and Utpal Dave and Susan Cleveland for helpful discussions. We thank Jonathan Keller (NCI) for the *Id1* and *Id2* expression plasmids, Juan-Carlos Zuniga-Pflucker (University of Toronto) for the OP9-DL1 cells, Robert Roeder (The Rockefeller University) for the E-box luciferase plasmid, and T. Ikawa and C. Murre (UCSD) for the E47-ER and Notch gene expression data sets. We thank the Vanderbilt-Ingram Cancer Center (P30CA68485) and the Vanderbilt Digestive Diseases Research Center (5P30DK58404) for support and the use of shared resources, including flow cytometry, functional genomics/microarrays, transgenic/embryonic stem cells, and human tissue acquisition and pathology.

This work was supported by National Institutes of Health (NIH) grants R01-CA64140 (S.W.H.), R01-HL088494 (S.W.H.), and F30 HL093993 (A.H.).

REFERENCES

- Amann, J. M., et al. 2001. ETO, a target of t(8;21) in acute leukemia, makes distinct contacts with multiple histone deacetylases and binds mSin3A through its oligomerization domain. *Mol. Cell. Biol.* **21**:6470–6483.
- Bain, G., et al. 1997. E2A deficiency leads to abnormalities in alphabeta T-cell development and to rapid development of T-cell lymphomas. *Mol. Cell. Biol.* **17**:4782–4791.
- Bain, G., et al. 1994. E2A proteins are required for proper B cell development and initiation of immunoglobulin gene rearrangements. *Cell* **79**:885–892.
- Bain, G., M. W. Quong, R. S. Soloff, S. M. Hedrick, and C. Murre. 1999. Thymocyte maturation is regulated by the activity of the helix-loop-helix protein, E47. *J. Exp. Med.* **190**:1605–1616.
- Barndt, R., M. F. Dai, and Y. Zhuang. 1999. A novel role for HEB downstream or parallel to the pre-TCR signaling pathway during alpha beta thymopoiesis. *J. Immunol.* **163**:3331–3343.

6. **Benezra, R., R. L. Davis, D. Lockshon, D. L. Turner, and H. Weintraub.** 1990. The protein Id: a negative regulator of helix-loop-helix DNA binding proteins. *Cell* **61**:49–59.
7. **Bhalla, S., et al.** 2008. Differential roles for the E2A activation domains in B lymphocytes and macrophages. *J. Immunol.* **180**:1694–1703.
8. **Blobel, G. A.** 2000. CREB-binding protein and p300: molecular integrators of hematopoietic transcription. *Blood* **95**:745–755.
9. **Cai, Y., et al.** 2009. Eto2/MTG16 and MTGR1 are heteromeric corepressors of the TAL1/SCL transcription factor in murine erythroid progenitors. *Biochem. Biophys. Res. Commun.* **390**:295–301.
10. **Chyla, B. J., et al.** 2008. Deletion of Mtg16, a target of t(16;21), alters hematopoietic progenitor cell proliferation and lineage allocation. *Mol. Cell. Biol.* **28**:6234–6247.
11. **Cochrane, S. W., Y. Zhao, R. S. Welner, and X. H. Sun.** 2009. Balance between Id and E proteins regulates myeloid-versus-lymphoid lineage decisions. *Blood* **113**:1016–1026.
12. **Corpora, T., et al.** 2010. Structure of the AML1-ETO NHR3-PKA(RIIalpha) complex and its contribution to AML1-ETO activity. *J. Mol. Biol.* **402**:560–577.
13. **Dias, S., R. Mansson, S. Gurbuxani, M. Sigvardsson, and B. L. Kee.** 2008. E2A proteins promote development of lymphoid-primed multipotent progenitors. *Immunity* **29**:217–227.
14. **Engel, M. E., H. N. Nguyen, J. Mariotti, A. Hunt, and S. W. Hiebert.** Myeloid translocation gene 16 (MTG16) interacts with Notch transcription complex components to integrate Notch signaling in hematopoietic cell fate specification. *Mol. Cell. Biol.* **30**:1852–1863.
15. **Erickson, P., et al.** 1992. Identification of breakpoints in t(8;21) acute myelogenous leukemia and isolation of a fusion transcript, AML1/ETO, with similarity to *Drosophila* segmentation gene, runt. *Blood* **80**:1825–1831.
16. **Fukuyama, T., et al.** 2001. MTG8 proto-oncoprotein interacts with the regulatory subunit of type II cyclic AMP-dependent protein kinase in lymphocytes. *Oncogene* **20**:6225–6232.
17. **Gamou, T., et al.** 1998. The partner gene of AML1 in t(16;21) myeloid malignancies is a novel member of the MTG8(ETO) family. *Blood* **91**:4028–4037.
18. **Gitmetti, V., et al.** 1998. Aberrant recruitment of the nuclear receptor corepressor-histone deacetylase complex by the acute myeloid leukemia fusion partner ETO. *Mol. Cell. Biol.* **18**:7185–7191.
19. **Goardon, N., et al.** 2006. ETO2 coordinates cellular proliferation and differentiation during erythropoiesis. *EMBO J.* **25**:357–366.
20. **Guo, C., Q. Hu, C. Yan, and J. Zhang.** 2009. Multivalent binding of the ETO corepressor to E proteins facilitates dual repression controls targeting chromatin and the basal transcription machinery. *Mol. Cell. Biol.* **29**:2644–2657.
21. **Ikawa, T., H. Kawamoto, A. W. Goldrath, and C. Murre.** 2006. E proteins and Notch signaling cooperate to promote T cell lineage specification and commitment. *J. Exp. Med.* **203**:1329–1342.
22. **Ikawa, T., H. Kawamoto, L. Y. Wright, and C. Murre.** 2004. Long-term cultured E2A-deficient hematopoietic progenitor cells are pluripotent. *Immunity* **20**:349–360.
23. **Jepsen, K., et al.** 2000. Combinatorial roles of the nuclear receptor corepressor in transcription and development. *Cell* **102**:753–763.
24. **Kee, B. L., G. Bain, and C. Murre.** 2002. IL-7Ralpha and E47: independent pathways required for development of multipotent lymphoid progenitors. *EMBO J.* **21**:103–113.
25. **Kitabayashi, I., et al.** 1998. The AML1-MTG8 leukemic fusion protein forms a complex with a novel member of the MTG8(ETO/CDR) family, MTGR1. *Mol. Cell. Biol.* **18**:846–858.
26. **Kovall, R. A.** 2008. More complicated than it looks: assembly of Notch pathway transcription complexes. *Oncogene* **27**:5099–5109.
27. **Laios, C. V., M. Stadtfeld, and T. Graf.** 2006. Determinants of lymphoid-myeloid lineage diversification. *Annu. Rev. Immunol.* **24**:705–738.
28. **Liu, Y., et al.** 2006. The tetramer structure of the Nrvy homology two domain, NHR2, is critical for AML1/ETO's activity. *Cancer Cell* **9**:249–260.
29. **Luc, S., N. Buza-Vidas, and S. E. Jacobsen.** 2008. Delineating the cellular pathways of hematopoietic lineage commitment. *Semin. Immunol.* **20**:213–220.
30. **Lutterbach, B., D. Sun, J. Schuetz, and S. W. Hiebert.** 1998. The MYND motif is required for repression of basal transcription from the multidrug resistance 1 promoter by the t(8;21) fusion protein. *Mol. Cell. Biol.* **18**:3604–3611.
31. **Lutterbach, B., et al.** 1998. ETO, a target of t(8;21) in acute leukemia, interacts with the N-CoR and mSin3 corepressors. *Mol. Cell. Biol.* **18**:7176–7184.
32. **Mansson, R., et al.** 2007. Molecular evidence for hierarchical transcriptional lineage priming in fetal and adult stem cells and multipotent progenitors. *Immunity* **26**:407–419.
33. **Miyoshi, H., et al.** 1993. The t(8;21) translocation in acute myeloid leukemia results in production of an AML1-MTG8 fusion transcript. *EMBO J.* **12**:2715–2721.
34. **Moore, A. C., et al.** 2008. Myeloid translocation gene family members associate with T-cell factors (TCFs) and influence TCF-dependent transcription. *Mol. Cell. Biol.* **28**:977–987.
35. **Plevin, M. J., J. Zhang, C. Guo, R. G. Roeder, and M. Ikura.** 2006. The acute myeloid leukemia fusion protein AML1-ETO targets E proteins via a paired amphipathic helix-like TBP-associated factor homology domain. *Proc. Natl. Acad. Sci. U. S. A.* **103**:10242–10247.
36. **Radtke, F., et al.** 1999. Deficient T cell fate specification in mice with an induced inactivation of Notch1. *Immunity* **10**:547–558.
37. **Rice, K. L., I. Hormaeche, and J. D. Licht.** 2007. Epigenetic regulation of normal and malignant hematopoiesis. *Oncogene* **26**:6697–6714.
38. **Salat, D., R. Liefke, J. Wiedenmann, T. Borggreffe, and F. Oswald.** 2008. ETO, but not leukemogenic fusion protein AML1/ETO, augments RBP-Jkappa/SHARP-mediated repression of notch target genes. *Mol. Cell. Biol.* **28**:3502–3512.
39. **Schmitt, T. M., and J. C. Zuniga-Pflucker.** 2002. Induction of T cell development from hematopoietic progenitor cells by delta-like-1 in vitro. *Immunity* **17**:749–756.
40. **Schotte, R., et al.** 2010. Synergy between IL-15 and Id2 promotes the expansion of human NK progenitor cells, which can be counteracted by the E protein HEB required to drive T cell development. *J. Immunol.* **184**:6670–6679.
41. **Schuh, A. H., et al.** 2005. ETO-2 associates with SCL in erythroid cells and megakaryocytes and provides repressor functions in erythropoiesis. *Mol. Cell. Biol.* **25**:10235–10250.
42. **Schwartz, R., I. Engel, M. Fallahi-Sichani, H. T. Petrie, and C. Murre.** 2006. Gene expression patterns define novel roles for E47 in cell cycle progression, cytokine-mediated signaling, and T lineage development. *Proc. Natl. Acad. Sci. U. S. A.* **103**:9976–9981.
43. **Semerad, C. L., E. M. Mercer, M. A. Inlay, I. L. Weissman, and C. Murre.** 2009. E2A proteins maintain the hematopoietic stem cell pool and promote the maturation of myelolymphoid and myeloerythroid progenitors. *Proc. Natl. Acad. Sci. U. S. A.* **106**:1930–1935.
44. **Sun, X. H., N. G. Copeland, N. A. Jenkins, and D. Baltimore.** 1991. Id proteins Id1 and Id2 selectively inhibit DNA binding by one class of helix-loop-helix proteins. *Mol. Cell. Biol.* **11**:5603–5611.
45. **Wei, Y., et al.** 2007. A TAF4-homology domain from the corepressor ETO is a docking platform for positive and negative regulators of transcription. *Nat. Struct. Mol. Biol.* **14**:653–661.
46. **Yan, M., et al.** 2006. A previously unidentified alternatively spliced isoform of t(8;21) transcript promotes leukemogenesis. *Nat. Med.* **12**:945–949.
47. **Yang, Q., B. Esplin, and L. Borghesi.** 2011. E47 regulates hematopoietic stem cell proliferation and energetics but not myeloid lineage restriction. *Blood* **117**:3529–3538.
48. **Zhang, J., M. Kalkum, S. Yamamura, B. T. Chait, and R. G. Roeder.** 2004. E protein silencing by the leukemogenic AML1-ETO fusion protein. *Science* **305**:1286–1289.